

Performance of Seismic Arrays in the Presence of Weathering Layer Variations*

Jubran Akram¹ and Abdullatif A. Al-Shuhail²

Search and Discovery Article #41841 (2016)

Posted September 12, 2016

*Adapted from extended abstract prepared in relation to poster presentation and from the presentation itself given at GEO 2016, 12th Middle East Geosciences Conference & Exhibition, Manama, Bahrain, March 7-10, 2016

¹Zero-Offset Technology Solutions, Canada (jubran.akram@zero-offsets.com)

²King Fahd University of Petroleum and Minerals, Saudi Arabia (ashuhail@kfupm.edu.sa)

Abstract

Near-surface layer variations can degrade the desired response of seismic arrays, which are typically used to attenuate horizontally traveling coherent noise and enhance vertically traveling signal. We investigate the effect of variations in the near-surface layer thickness on the performance of arrays by studying their impulse and wavelet responses. The models considered include the topographic variations and a channel in the base of weathering layer. The topographic variations include a dipping surface layer as well as a surface layer that follows a sine wave. The geological channel is assumed present under the entire receiver array as well as partially under a few receivers. We use Ricker wavelet and model plane wavefronts with incidence angles (90°, 70°, 45°, 20° and 5°) on a 12-element equally weighted array for the weathering layer models. We found that the array responses are more degraded for near-vertically travelling waves in all cases. The array responses are also found to be more degraded when channel variations are present underneath a few receivers as compared to the entire array length.

Introduction

A receiver array response is defined as the sum of outputs of the individual receivers comprising the array. It measures the ability of receiver array to attenuate noise and pass the desired signals without distortion (Al-Shuhail, 2011). Under typical field conditions, a variety of factors influences the response of receiver arrays. This results in differences from the nominal response associated with ideal conditions such as precise positioning, vertical plants, identical geophones and perfect ground coupling (Aldridge, 1989). In many onshore exploration areas, the land surface is covered with a relatively thin layer of material of low seismic velocity. Variations in thickness and velocity of the near-surface layers can also alter the receiver response and deteriorate the quality of land seismic data if the problem is ignored during data acquisition and processing (Pritchett, 1989; Marsden, 1993).

In this paper, we assess the impact of variations in near-surface layer thickness on the performance of receiver arrays by studying their impulse and wavelet responses. The near-surface models considered include both topographic variations and a channel in the base of weathering layer. We use Ricker wavelet and model plane wavefronts with incidence angles (90°, 70°, 45°, 20° and 5°) on a 12-element equally weighted array

for 4 different thickness variation models 1) A dipping surface layer and a channel present at the base of weathering layer under the entire array 2) Surface layer topography follows sine wave and a channel is present at the base of weathering layer under the entire array 3) A dipping surface layer and a channel present at the base of weathering layer partially under the array 4) Surface layer topography follows sine wave and a channel is present at the base of weathering layer partially under the receiver array.

Methodology

The methodology is described as follows (Al-Shuhail, 2011):

- Impulse and wavelet responses of the receiver array are computed for an ideal case (no thickness variation in the weathering layer).
- The normalized maximum RMS amplitudes of the wavelet response are computed over an optimum window.
- Perturbed array responses are generated for the assumed model that simulates the effect of near-surface thickness variations on the receiver array
- The maximum RMS amplitudes of the perturbed wavelet responses are analysed.

For an ideal weathering layer model (no thickness variation), the impulse response of the receiver array is computed as

$$I(Y, \tau; \tau^*) = \sum_{n=0}^{N-1} W(y_n) \delta(\tau - \tau_n), \quad (1)$$

where y_n is the normalized location of n^{th} receiver, W is the weighting function, N is the number of receivers comprising the array, τ is the normalized traveltme and τ^* is the normalized total traveltme across the array. The wavelet response of the receiver array is

$$G(Y, \tau; \tau^*) = I(Y, \tau; \tau^*) * u(\tau) = \sum_{n=0}^{N-1} W(y_n) u(\tau - \tau_n), \quad (2)$$

where u is the Ricker wavelet. Finally, the RMS amplitude response over a window of width τ_w is

$$S(j, \tau_w; \tau^*) = \sqrt{\frac{1}{w} \sum_{i=j}^{j+w} G^2(Y, i; \tau^*)}, \quad (3)$$

where j is the first sample of the window, w is the number of samples in the window and $G(Y; i; \tau^*)$ is the amplitude of the sample of the wavelet response at point i . The normalized maximum RMS amplitude of the wavelet response of receiver array is then computed as

$$r(\tau_w; \tau^*) = \frac{\max[S(j, \tau_w; \tau^*)]}{\max[S(j, \tau_w; 0)]}. \quad (4)$$

where \max indicates the maximum value of the RMS-amplitude found over the whole trace. In decibel (dB) scale, the normalized maximum RMS amplitude is

$$R(\tau_w; \tau^*) = 20 \log_{10} r(\tau_w; \tau^*). \quad (5)$$

[Figure 1](#) shows one of the models considered in this paper in which surface layer is dipping with an angle α and a geological channel exists underneath the entire receiver array at the base of weathering layer. For this case, the total travel time for the n^{th} receiver becomes

$$\tau_{tot} = \tau + \Delta\tau_e = \frac{n\Delta x \sin \theta}{V_w T_{dom}} + \frac{n\Delta x \sin \alpha + b \sin \beta}{V_w T_{dom} \cos \theta}, \quad (6)$$

where Δx is the receiver spacing prior to normalization, T_{dom} is the dominant period of the wavelet, θ is the incidence angle of the plane wavefront, V_w is the weathering layer velocity, b is the channel depth, and β is the angle of the line connecting the intersection point of ray at the channel (weathering layer) base to the center of channel. τ_{tot} equals the ideal travel time equation in the absence of a dipping surface layer and geological channel. Similarly, the total travel times are computed for other perturbed models.

Results

In the first case, the surface layer is dipping at an angle 10° whereas a geological channel is present at the base of weathering layer under the entire array ([Figure 1](#)). The channel depth and the ideal thickness of the weathering layer are assumed to be 7m and 150m, respectively. [Figure 2](#) shows the RMS amplitude response in the presence of such variations in weathering layer thickness. The incident angles near to horizontal are least affected by such thickness variations and yield amplitude responses which are identical to the ideal response. The amplitude response achieves higher values as $\tau^* \rightarrow 0$. Increasing τ^* results in a decrease of the RMS amplitude response of the receiver array until it attains a minimum value at $\tau^* = (N-1)/2 = 5.5$ (corresponding to a wavelet period of 0.03s). Ideally, this specific array is designed to attenuate 26Hz frequency component. The array responses for the incident angles $\theta = 70^\circ, 45^\circ, 20^\circ$ show very minor deviations from the ideal response. Despite the minimum value occurring near to τ^* obtained for gentle angles ($\theta = 90^\circ, 70^\circ, 45^\circ$), the RMS amplitude value is slightly higher which indicates lower performance of receiver array in attenuating the desired frequency from the incident wavelet. For $\theta = 5^\circ$, RMS amplitude response yields higher values as well as the minimum occurs at a different τ^* value which suggests that the receiver array will demonstrate poor attenuation for desired frequency component.

In case 2, the topographic variations of surface layer follow a sine wave whereas the channel variations are identical to those observed in the previous case. [Figure 3](#) shows the RMS amplitude response of 12-element receiver array for this case. For $\theta = 20^\circ$, the values of RMS amplitudes are higher as compared to the previous case. Higher degradation is observed in the RMS amplitude response for plane wavefront incident at $\theta = 5^\circ$ and as a result the receiver array will be unable to achieve the desired attenuation and signal enhancement.

In case 3 where surface layer is dipping and a channel is only present partially under the receiver array, the RMS amplitude response for $\theta = 20^\circ$ and 5° are more degraded ([Figure 4](#)). The degradation is not severe for $\theta = 70^\circ$ and 45° but for $\theta = 20^\circ$, degradation in RMS amplitude is higher as compared to the previous two cases.

[Figure 5](#) shows the RMS amplitude response curves for case 4 where surface layer follows a sine wave and a channel is only present partially under the receiver array. Similar to previous cases, the responses for near-vertical incident angles are more degraded. The RMS amplitude values for $\theta = 20^\circ$ show more degradation than in any previous cases. For $\theta = 5^\circ$, the RMS amplitude values are higher and the minimum value is observed at $\tau^* = 3.5$.

Conclusions

We have assessed the performance of seismic arrays in the presence of weathering layer thickness variations by studying the impulse and wavelet responses. We have investigated four different models of weathering layer variations. The perturbation in the surface layer topography (dipping surface as well as a surface layer that resembles a sine wave) and a channel at the base of weathering layer is considered. We have used Ricker wavelet and modeled plane wavefronts with incidence angles (90° , 70° , 45° , 20° and 5°) on a 12-element equally weighted array for the weathering layer models. The variation in weathering layer thickness degrades the amplitude response of the receiver array. We found that wavefronts travelling horizontally are least affected by the changes in weathering layer thickness whereas the vertically travelling waves are severely impacted by such changes. The RMS amplitude response becomes higher and maximum attenuation is yielded at higher τ^* which suggests poor attenuation of the desired frequency from the incident wavelet. Our results also indicate that array responses undergo higher degradation when the channel is present partially under the receiver array and when the surface layer topography resembles a sine wave. Such degradation in the receiver array response also affects the reflection amplitudes, which can lead to errors in interpretation.

References Cited

- Aldridge, D.F., 1989, Statistically perturbed geophone array responses: *Geophysics*, v. 54, p. 1306-1318.
- Al-Shuhail, A., 2011, Seismic array response in the presence of a dipping shallow layer: *SIViP*, v. 7, p. 263-274.
- Marsden, D., 1993, Static corrections: a review: *The Leading Edge*, v. 12, p. 43-49.
- Pritchett, W.C., 1989, *Acquiring Better Seismic Data*: Chapman and Hall.

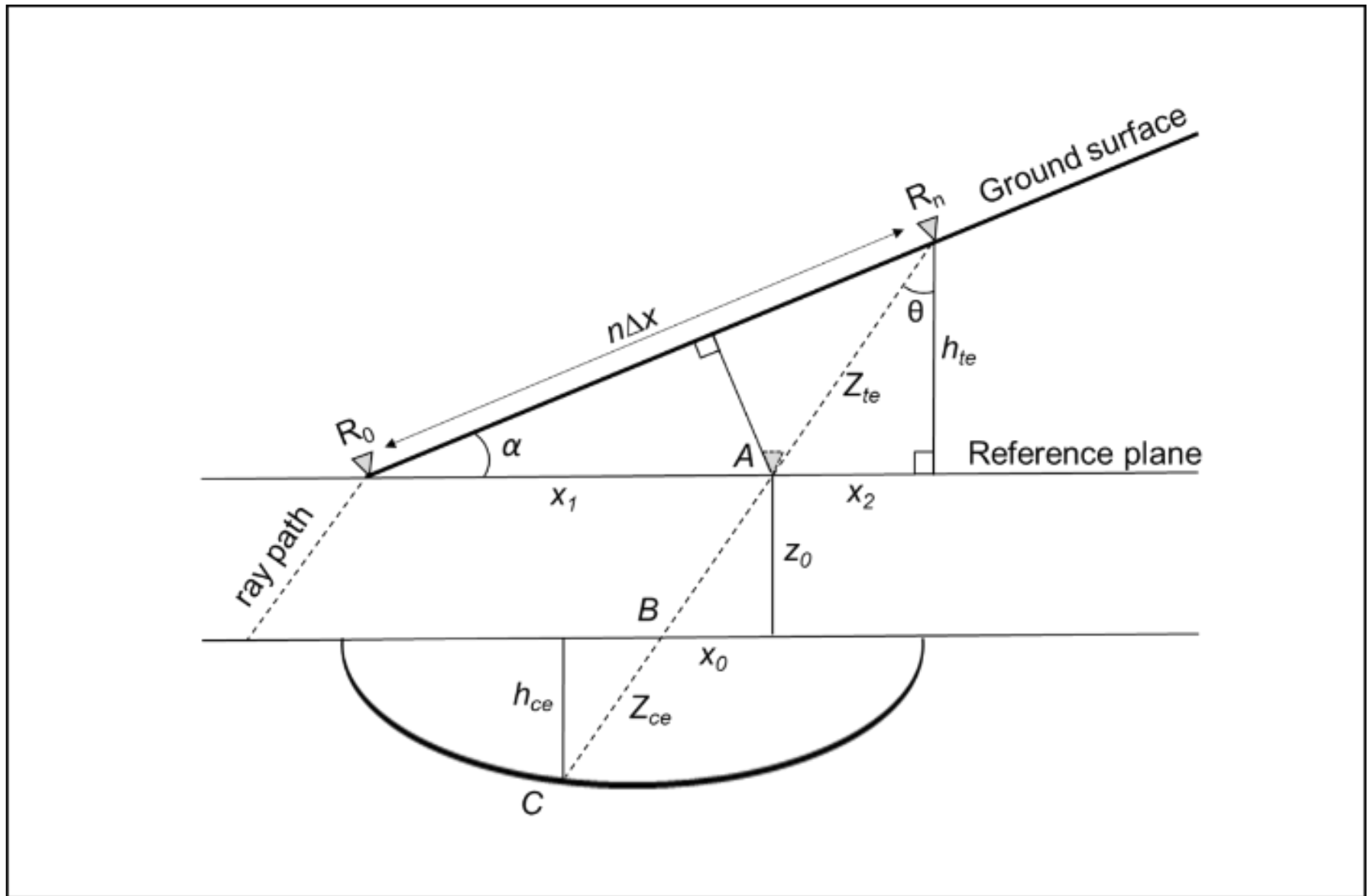


Figure 1. An example of travel time error calculation for one of the cases of weathering layer thickness variations considered here. The surface layer is dipping whereas there exists a geological channel at the base of weathering layer. The plane wavefront is incident at an angle θ .

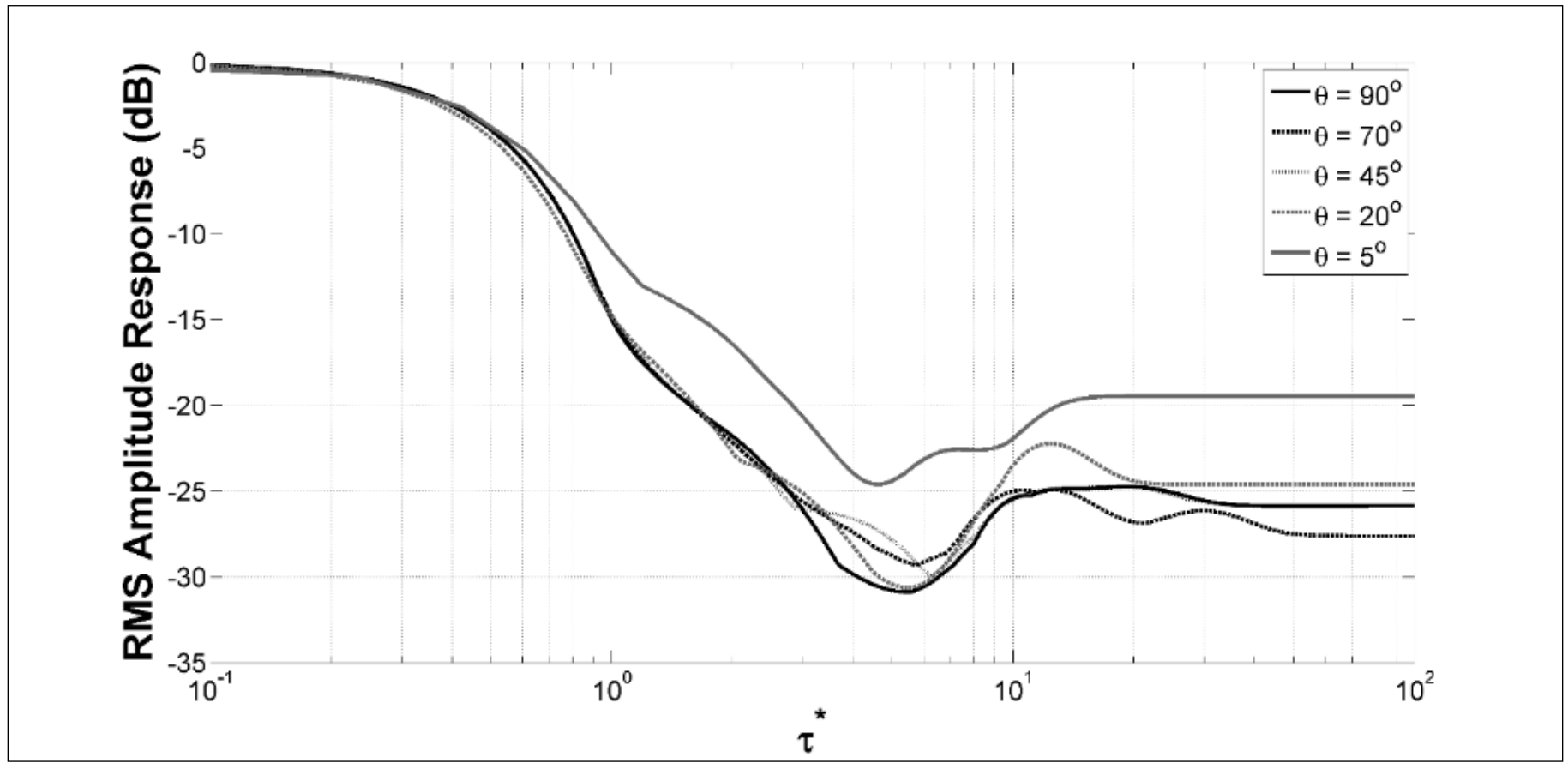


Figure 2. RMS amplitude responses for plane wavefronts incident at $\theta = 90^\circ$, 70° , 45° , 20° and 5° for weathering layer thickness variations (case 1). In this case, surface layer is dipping at 10° and a channel is present at the base of weathering layer spanning the entire array length.

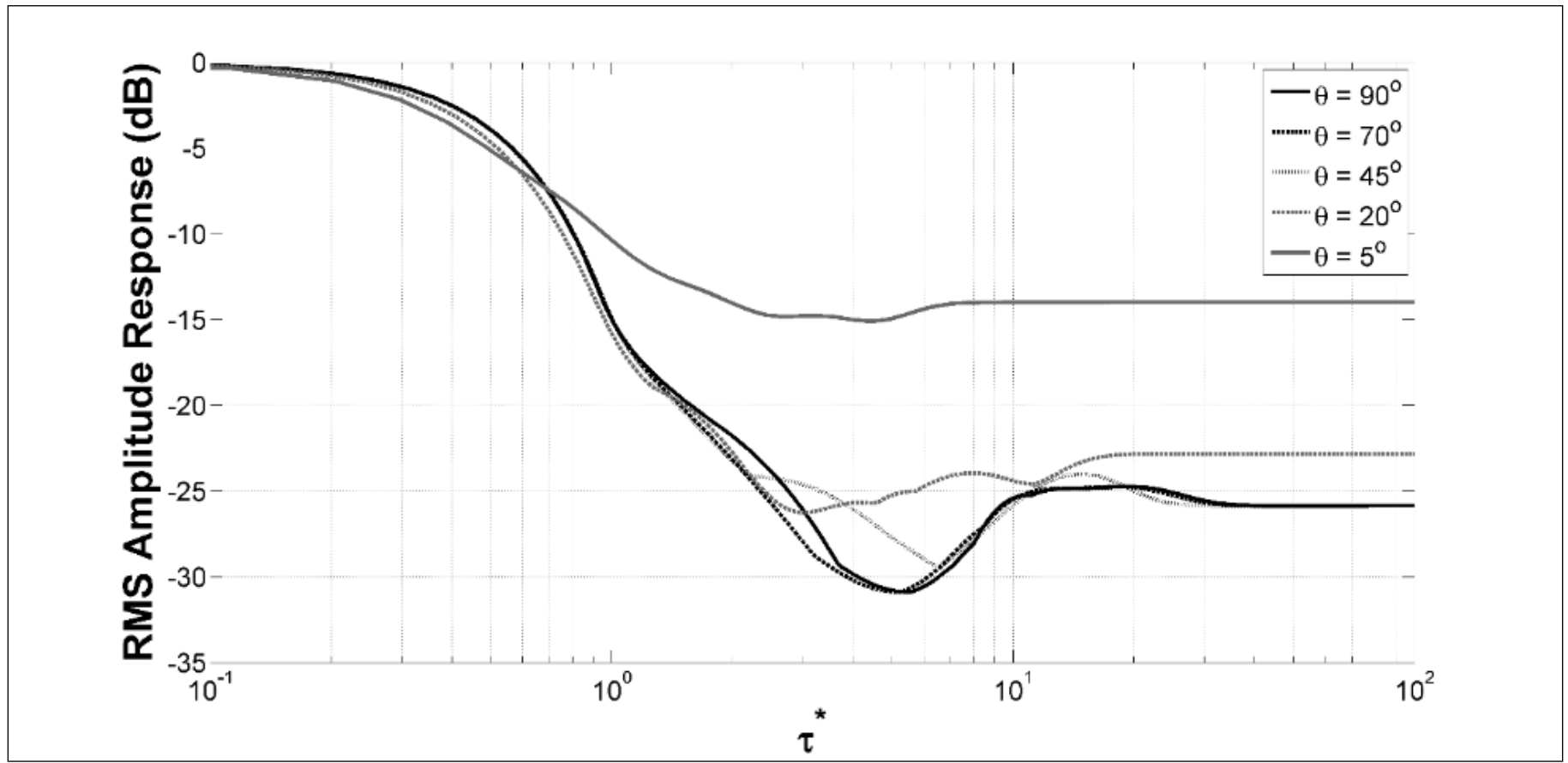


Figure 3. RMS amplitude responses for plane wavefronts incident at $\theta = 90^\circ$, 70° , 45° , 20° and 5° for weathering layer thickness variations (case 2). In this case, surface layer resembles a sine wave and a channel is present at the base of weathering layer spanning the entire array length.

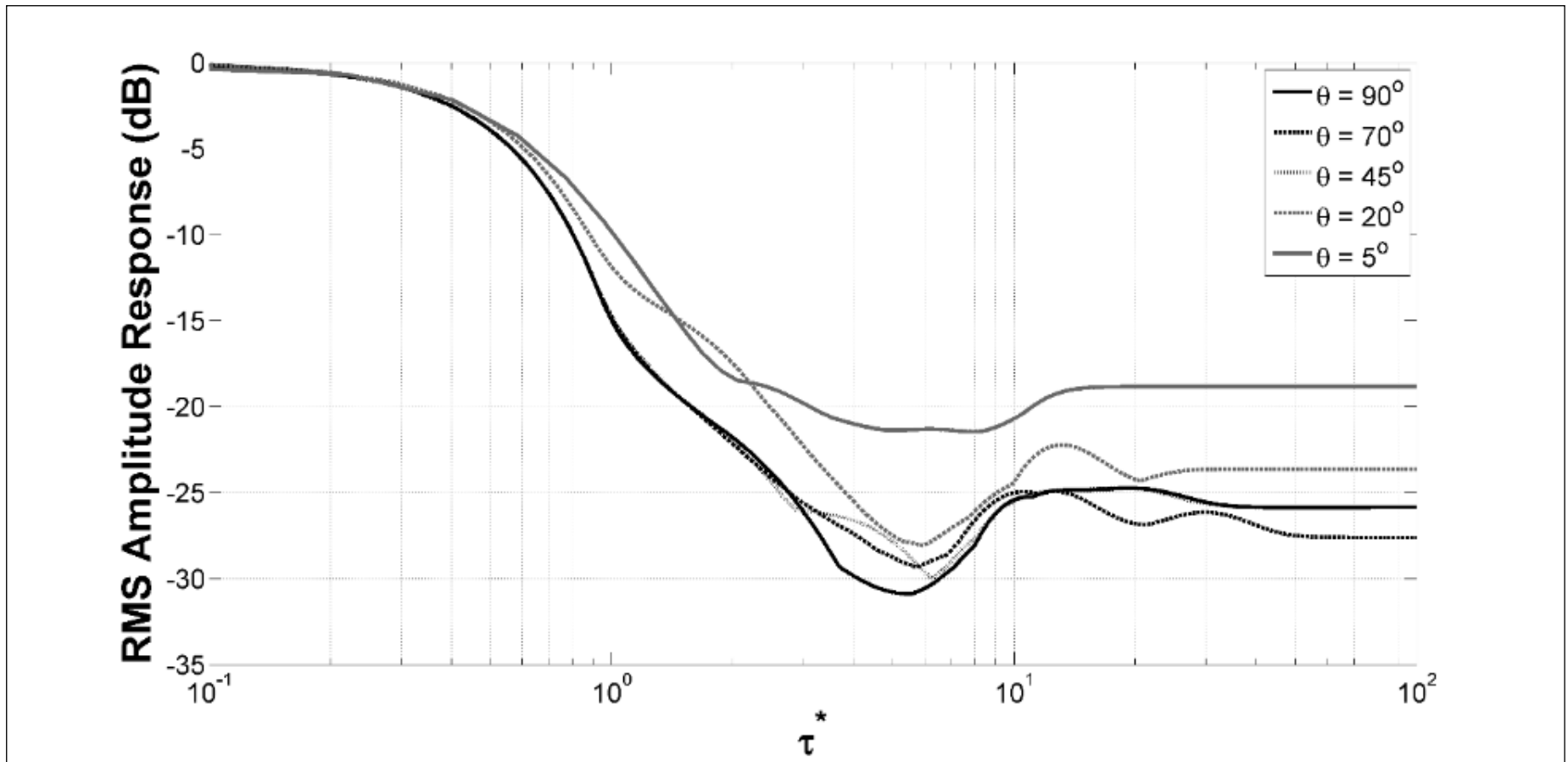


Figure 4. RMS amplitude responses for plane wavefronts incident at $\theta = 90^\circ$, 70° , 45° , 20° and 5° for weathering layer thickness variations (case 3). In this case, surface layer dipping at 10° and a channel is present at the base of weathering layer partially under the array.

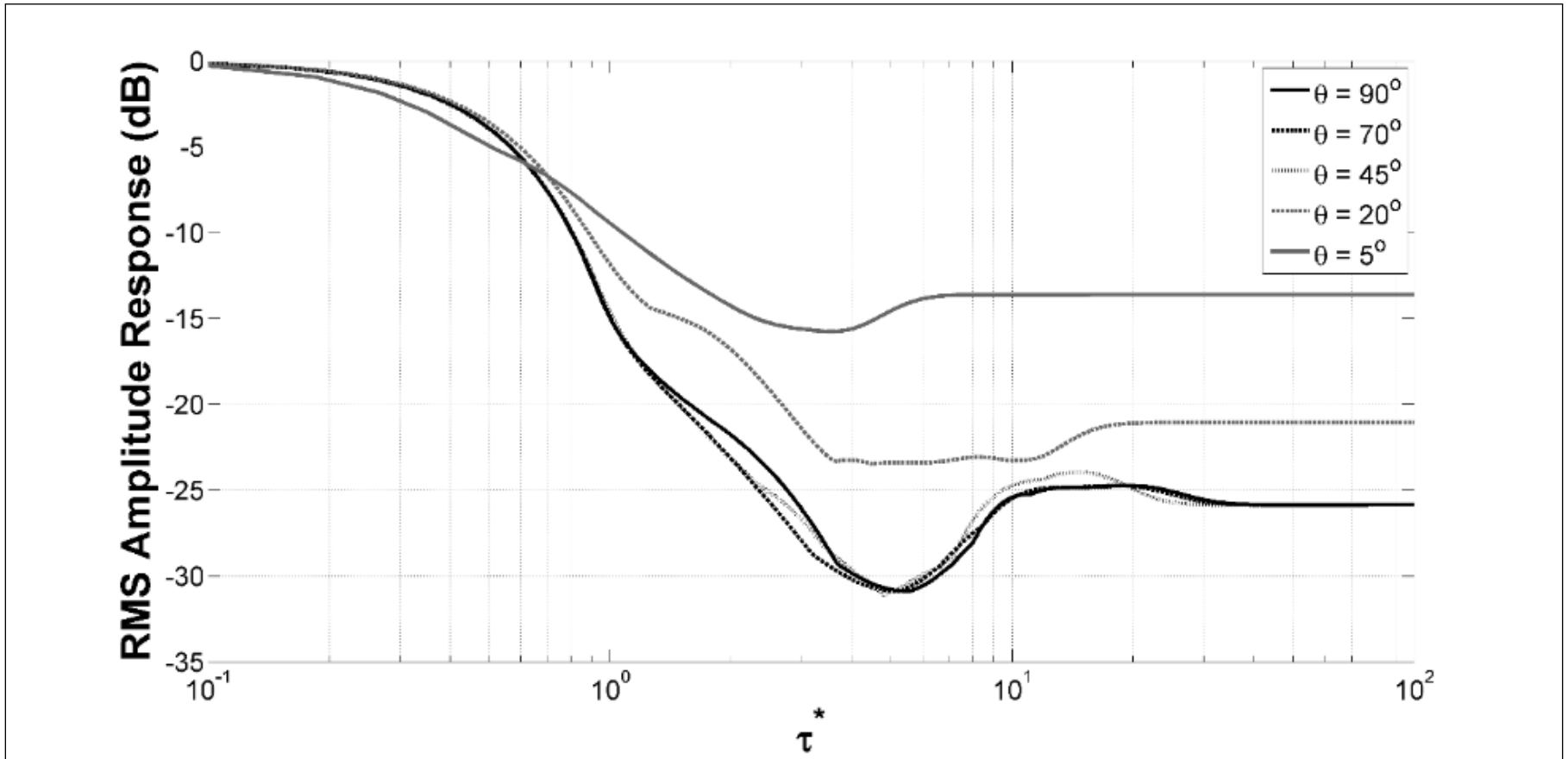


Figure 5. RMS amplitude responses for plane wavefronts incident at $\theta = 90^\circ$, 70° , 45° , 20° and 5° degrees for weathering layer thickness variations (case 4). In this case, surface layer resembles a sine wave and a channel is present at the base of weathering layer partially under the array.